The Knee 41 (2023) 9–17

Contents lists available at ScienceDirect

The Knee

journal homepage:

Fully automatic extraction of knee kinematics from dynamic CT imaging; normative tibiofemoral and patellofemoral kinematics of 100 healthy volunteers

Hans Dunning [a,*], S.A.W. van de Groes [b], C.F. Buckens [d], Mathias Prokop [d], Nico Verdonschot [a,c], Dennis Janssen [a]

[a] Orthopaedic Research Laboratory, Radboud Institute for Health Sciences, Radboud University Medical Center, Nijmegen, the Netherlands
[b] Department of Orthopaedics, Radboud University Medical Center, Nijmegen, the Netherlands
[c] University of Twente, Laboratory for Biomechanical Engineering, Faculty of Engineering Technology, Enschede, the Netherlands
[d] Department of Radiology, Radboud University Medical Center, Nijmegen, the Netherlands

ARTICLE INFO

Article history:
Received 8 September 2022
Revised 23 October 2022
Accepted 14 December 2022

Keywords:
Knee kinematics
Patellofemoral joint
Tibiofemoral joint
Dynamic Imaging
4DCT

ABSTRACT

Background: Accurate assessment of knee kinematics is important in the diagnosis and quantification of knee disorders and to determine the effect of orthopaedic interventions. Despite previous studies showing the usefulness of dynamic imaging and providing valuable insights in knee kinematics, dynamic imaging is not widely used in clinics due to a variety of causes. In this study normative knee kinematics of 100 healthy subjects is established using a fully automatic workflow feasible for use in the clinic.
Methods: One-hundred volunteers were recruited and a dynamic CT scan was made during a flexion extension movement. Image data was automatically segmented and dynamic and static images were superimposed using image registration. Coordinate systems for the femur, patella and tibia were automatically calculated as well as their dynamic position and orientation.
Results: Dynamic CT scans were made with an effective radiation dose of 0.08 mSv. The median tibial internal rotation was 4° and valgus rotation is 5° at full flexion. Femoral rollback of the lateral condyle was 7 mm versus 2 mm of the medial condyle. The median patella flexion reached 65% of tibiofemoral flexion and the median tilt and rotation were 5° and 0° at full flexion, respectively. The median mediolateral translation of the patella was 3 mm (medially) in the first 30° of flexion.
Conclusion: The current study presents TF and PF kinematic data of 97 healthy individuals, providing a unique dataset of normative knee kinematics. The short scanning time, simple motion and, automatic analysis make the methods presented suitable for daily clinical practice.
© 2022 The Author(s). Published by Elsevier B.V. This is an open access article under the CC BY license (http://creativecommons.org/licenses/by/4.0/).

* Corresponding author at: Radboud University Medical Center, P.O. Box 9101, 6500 HB Nijmegen (620), the Netherlands.
E-mail address: hans.dunning@radboudumc.nl (H. Dunning).

https://doi.org/10.1016/j.knee.2022.12.011
0968-0160/© 2022 The Author(s). Published by Elsevier B.V.
This is an open access article under the CC BY license (http://creativecommons.org/licenses/by/4.0/).

1. Introduction

Knee disorders such as ligament injury or patellofemoral instability affect the dynamic functioning of the knee joint. Accurate assessment of knee kinematics is therefore important in the diagnosis and quantification of such disorders, and to determine the effect of orthopaedic interventions. Current diagnostic imaging in clinical practice, however, is predominantly taken while the subject is in passive, supine position. During imaging, potential important information on the effect of joint motion and the influence of soft tissues such as ligaments, tendons and muscles is thereby not captured [1]. To assess the potential added information during dynamic scanning, there is a need for objective and accurate determination of subject-specific knee kinematics, and the possibility of comparing them with normative kinematics, in a clinical setting.

In order to diagnose subject-specific knee kinematics and pathologies, several in-vivo dynamic imaging techniques of the knee joint have been developed using a variety of different modalities such as MRI, Fluoroscopy, CT or a combination of these techniques [1,2]. In these studies various loading conditions and dynamic tasks were investigated [3–6]. Unfortunately, these studies mainly focus on patellofemoral kinematics (PF) and very rarely the combination of tibiofemoral (TF) and PF kinematics, while these are known to influence each other [7].

In two comprehensive review studies, the current state of dynamic imaging for the patellofemoral joint was studied [2,8]. Both review studies conclude that dynamic imaging provides valuable insight into knee kinematics and pathologies and underline the need for objective and accurate determination of subject-specific knee kinematics. However, these studies also reveal a number of limitations that need to be addressed before implementation of dynamic imaging in general clinical practice is possible. For instance, due to differences in modalities, loading conditions, range of motion, and analysis methods it is difficult to compare and generalise dynamic imaging studies. Secondly, practical limitations such as time consuming scanning sequences in case of dynamic MRI require intensive coordination and cooperation of the patient. Thirdly, dynamic imaging provides a multitude of data compared to conventional static imaging, rendering manual assessment by a radiologist too time-consuming, and is prone to variabilities that complicate intra- and intersubject comparison.

To overcome these limitations, a fully automatic analysis method was developed that is able to simultaneously extract tibiofemoral and patellofemoral kinematics from dynamic CT imaging. The short duration and simplicity (no loading rigs, or moving frequency required) of the scan protocol and automatic segmentation and kinematic quantification allows for use in daily clinical practice and ensures fast and consistent determinations of knee kinematics. In the current study we used this method to determine PF and TF kinematics in a cohort of 100 healthy subjects, with the objective to establish normative knee kinematics from dynamic CT imaging that can be used as a baseline dataset in future clinical studies investigating various types of knee joint pathology.

2. Methods

Prior to the current study, a dose reduction study was performed to ensure the radiation dose was below the maximum limit for healthy volunteers (protocol dose 0.08 mSv). Institutional approval was obtained to perform a dynamic CT scan on healthy volunteers. One-hundred volunteers from the age of 18 years were included with a maximum of 35 years to avoid altered kinematics due to early onset arthrosis. Subjects were not allowed to have any previous knee pathologies, prior trauma or surgery to the knee. This was checked by briefly discussing their medical background regarding these subjects. Reports on dysfunction, pain or prior surgery were reason for exclusion. Further exclusion criteria were functional or congenital disorders and severe valgus or varus malalignment. The exclusion criteria were assessed by the first author during an intake interview. Sex, age and BMI of all participants were determined and recorded. All participants signed an informed consent form prior to participating.

A single high resolution static scan (voxel size $0.71 \times 0.71 \times 0.80$ mm) of both legs was made of the subject in supine position (Canon Aquilion One). The field of view was 500 mm and included the distal half of the femur, the proximal half of the tibia and the full patella. The subject was then moved to the end of the scanner table, and an angled pillow was placed in the popliteal fossa, with both legs hanging freely over the edge of the scanner table (see Figure 1). Subsequently, subjects were asked to assume a relaxed, semi-seated position, so the movement could be easily performed with minimal effort.

Figure 1. Overview of the scan protocol and corresponding CT images. a) a high resolution static scan is made of the patient in supine position on the scanner table. b&c) The subject is moved to the end of the scanner table and an angled pillow is placed in the popliteal fossa. The subject is asked to fully extend and flex both legs in approximately 10 s.

Subjects were asked to move both legs from approximately 90° of flexion to full extension and back again in approximately 10 s. The movement was practiced prior to the actual scan, so that a smooth and full extension-flexion movement was completed within the scanning time. During the dynamic scan, 41 images were made while the subject moved both knees. The field of view during dynamic scanning was 160 mm. A subject positioning protocol was used to ensure that the entire patella, and parts of the proximal tibia and the distal femur were continuously within the field of view during the scan. Prior validation studies have demonstrated that dynamic CT imaging is accurate ($\sim$1° and 1 mm of x,y,z rotation and translation) and comparable to other dynamic imaging techniques [9,10]. Given the high similarity in image acquisition, similar accuracies are expected in this study.

The left and right femur, patella, tibia and patellar tendon of all subjects were segmented with a deep learning network [11]. The deep learning algorithm had a DICE coefficient of 0.99 for the femur, 0.98 for the tibia and 0.96 for the patella compared to manual segmentations, demonstrating that the algorithm is capable of performing accurate and precise segmentations. Segmentation masks were automatically transformed into 3D surface meshes (MATLAB), and remeshed and smoothed without manual intervention, in order to improve mesh quality [12].

As the field of view of the dynamic scans is too small for accurate landmark and axes determination, the femur, patella and tibia of the static scans were superimposed by subsequent pointcloud- (Coherent Point Drift) and image-registration (Elastix 5.0.1) [13,14]. Although the accuracy of (image) registration is notoriously difficult to determine, the algorithms used in this study are well established and have demonstrated high accuracies and will likely introduce minimal inaccuracies. All spatial transformations were saved in an Elastix transform file. Coordinate Systems (CS) were calculated for every static femur, patella and tibia, similar to those described by Miranda et al. [15]. Each orthogonal coordinate system consisted of Superior-Inferior (SI), Anterior-Posterior (AP) and Medial-Lateral (ML) axis. The sensitivity of the coordinate system was determined in a previous publication, which concluded that with common anatomy, the kinematics of the knee can be described with acceptable certainty [16]. A detailed description of the calculation of the femoral and tibial coordinate systems can be found in Chen et al. [17]. Furthermore a detailed description of the calculation of the patellar coordinate system can be found in a previous publication [16].

The transformations found in the dynamic scans were applied to each relative coordinate system to calculate their dynamic position and orientation. The angles between SI, AP and ML axes of the femur, patella and tibia were calculated according to the sequence described by Grood & Suntay [18]. Rotations of the tibia and patella were all calculated with respect to the femur (i.e. the femur was fixed in space). As data were collected at even time intervals (fastest acquisition speed of the scanner) and subjects were allowed to move freely, images were taken at different knee flexion angles between subjects. Therefore, spherical linear interpolation was used to calculate the rotations of the patella and tibia with respect to the femur for every degree of tibiofemoral flexion. Similarly, for the interpolation of translations, piece-wise linear interpolation was used.

To counteract differences in angles as a result of anatomical variation, to objectively describe motion and to allow inter-subject comparison, any rotational and translational offsets were negated similar to Amis et al., who assumed all rotations and translations to be zero at full extension [19]. Therefore, the smallest tibiofemoral flexion angle was calculated for both knees for every subject. In that position, the direction of the AP and ML axes of the femur were copied to the patellar and tibial AP and ML axes which essentially negates any rotations for that specific TF flexion angle. The orientation of the SI axis (flexion angle) was left unaffected.

Femoral Rollback was calculated by projecting the femoral trans epicondylar axis on the tibial plateau, specifically the centroids of the medial and lateral condylar articulating surface that, when connected, make up the femoral ML axis.

Rollback was separately calculated for the medial and lateral condyle as the translation of the projected points, similar to the method by Gray et al. [20]. Lastly, the patellar mediolateral translation was calculated by calculating the distance between the patellar and femoral CS origin along the ML axis of the femur. Similar to the rotations, the mediolateral patellar translation and femoral rollback were negated at the smallest tibiofemoral flexion angle (i.e. in extension) [19].

An overview of how TF and PF rotations and translations were calculated can be found in Figure 2.

To ensure usefulness and smoothness while allowing maximal range of flexion angles, the median and percentiles were only calculated and visualized at flexion angles which at least 65% of all subjects were able to reach within the scan time. This percentage was iteratively determined by maximizing range of motion (ROM) and number of subjects reaching that ROM. At least 65% of the subjects were able to reach TF flexion angles of 6–85° during the extension movement. For the flexion movement, 65% of the subjects were able to reach TF flexion angles of 6–70°.

3. Results

One hundred healthy volunteers were successfully recruited, of which 71 were female and 29 were male. The mean age was 24 years with a standard deviation of 3.36 years. All subjects were in the age range of 18–34 years old. The mean BMI of all subjects was 19 ± 2.8. Forty-one images were made during 11.3 s of active movement, resulting in a framerate of 3.6 frames per second. The effective radiation dose associated with the scan protocol was 0.08 mSv.

Of the 100 dynamic CT datasets, three datasets showed substantial image artifacts which prohibited automatic segmentation and registration, and the data were therefore excluded. As both knees were scanned, a total of 197 knees

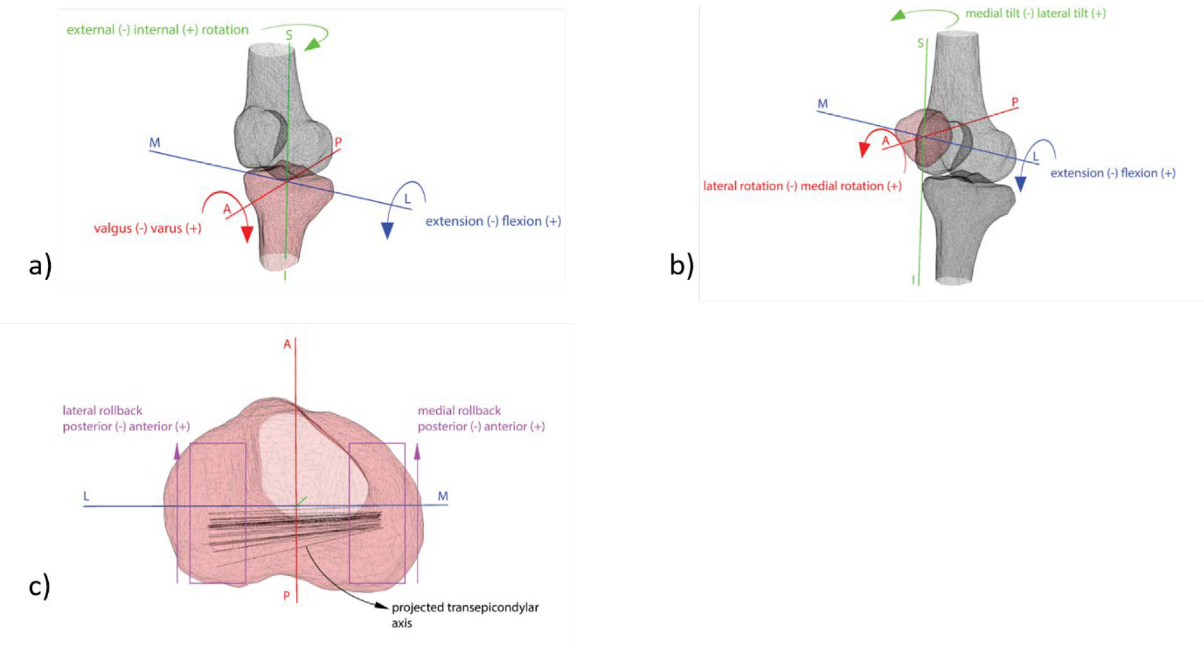

Figure 2. Overview of TF & PF rotations and femoral rollback. The example is a left knee. a) Tibiofemoral Rotations b) Patellofemoral rotations. Mediolateral patellar translation is measured along the ML axis of the femur. c) Femoral rollback is calculated by projecting the trans epicondylar axis of the femur onto the tibia plateau. The anterior and posterior movement is measured separately on the medial and lateral side.

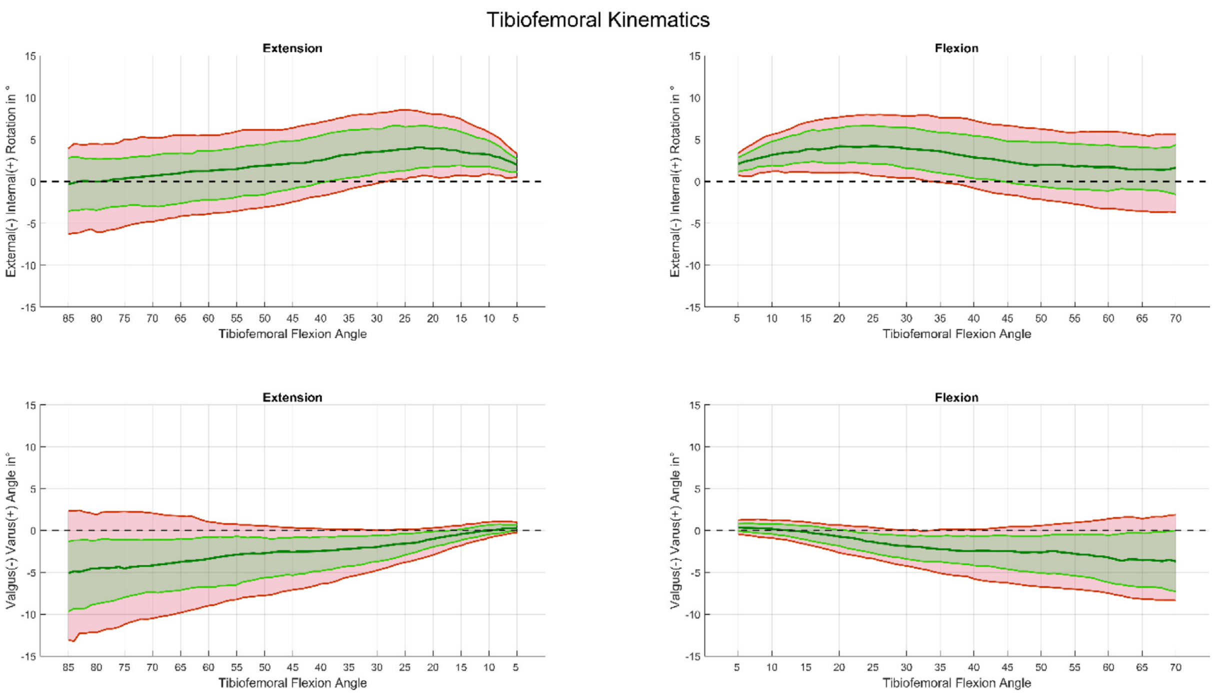

Figure 3a. Percentile plot of tibiofemoral kinematics during the extension-flexion movement, green line = media, green area = 25–50 percentile, red area = 12.5–87.5 percentile. Top = internal (−) external (+) rotation, bottom = Varus(−) Valgus(+) angle. (+). The horizontal axis contains the tibiofemoral flexion angle, the vertical axes are labelled. To ensure smoothness and readability of the plots, measurements are only displayed between 6° and 85° of flexion, as these angles were achieved by at least 65% of all subjects.

was analyzed. Remaining data was successfully segmented, registered and coordinate systems for the femur, patella and tibia were successfully calculated.

The median, 25–50 percentile and 12.5–87.5 percentile of tibiofemoral and patellofemoral kinematics are visualized in Figures 3 and 4. For visibility, the extension and flexion movements are visualized in separate subplots. The overall flexion range of all subjects was 3.37° ± 8.03° to 89.31° ± 8.78°.

There was a slight internal rotation of the tibia from 85° to approximately 30° of flexion, followed by external rotation from 30° to 6° of flexion. The variance between subjects was approximately 10° at larger flexion angles, and gradually decreased with lower flexion angles, resulting in a narrowing area between the percentiles plots. Both median and percentiles followed a slightly different path during the extension and flexion movement.

A small valgus angle of the tibia with respect to the femur was observed at higher flexion angles, which decreased with decreasing flexion angle. Similar to the internal external rotation, the variance in the measured varus-valgus angles was largest at higher flexion angles, with differences of ±15°, which became smaller with decreasing flexion angles. Both median and percentiles followed a slightly different path during the extension and flexion movement.

Femoral Rollback was largest at higher flexion angles, both medially and laterally. With decreasing flexion, rollback decreased. Femoral rollback overall was larger on the lateral side compared to the medial side. Both median and percentiles followed the same (inversed) path during the extension and flexion movement.

The median, 20–50 percentile and 12.5–87.5 percentile of medial and lateral femoral rollback and are visualized in Figure 3b.

Patellofemoral flexion reached approximately 2/3rd of tibiofemoral flexion throughout movement and patellar flexion decreased with decreasing tibiofemoral flexion. The variance was approximately 10° over the complete range of motion.

The patella was most laterally tilted at high TF flexion angles, which generally decreased with decreasing flexion. Patellar tilt remained roughly equal between 50° and 20° of TF flexion and decreased to zero nearing full extension. The variance was approximately 10° and decreased to 5° nearing full extension.

The patellar rotation was centred around 0° with a variance of approximately 10° at full flexion which decreased to 0° with decreasing TF flexion. The largest change in variance occurred at TF flexion angles larger than 30°.

The median, 20–50 percentile and 12.5–87.5 percentile of patellofemoral flexion, patellar tilt and patellar rotation are visualized in Figure 4a and Figure 4b.

The patella moved medially in the first 25° of TF flexion and remained stable after that. The median translation was ±2.5 mm and the variance ±10 mm.

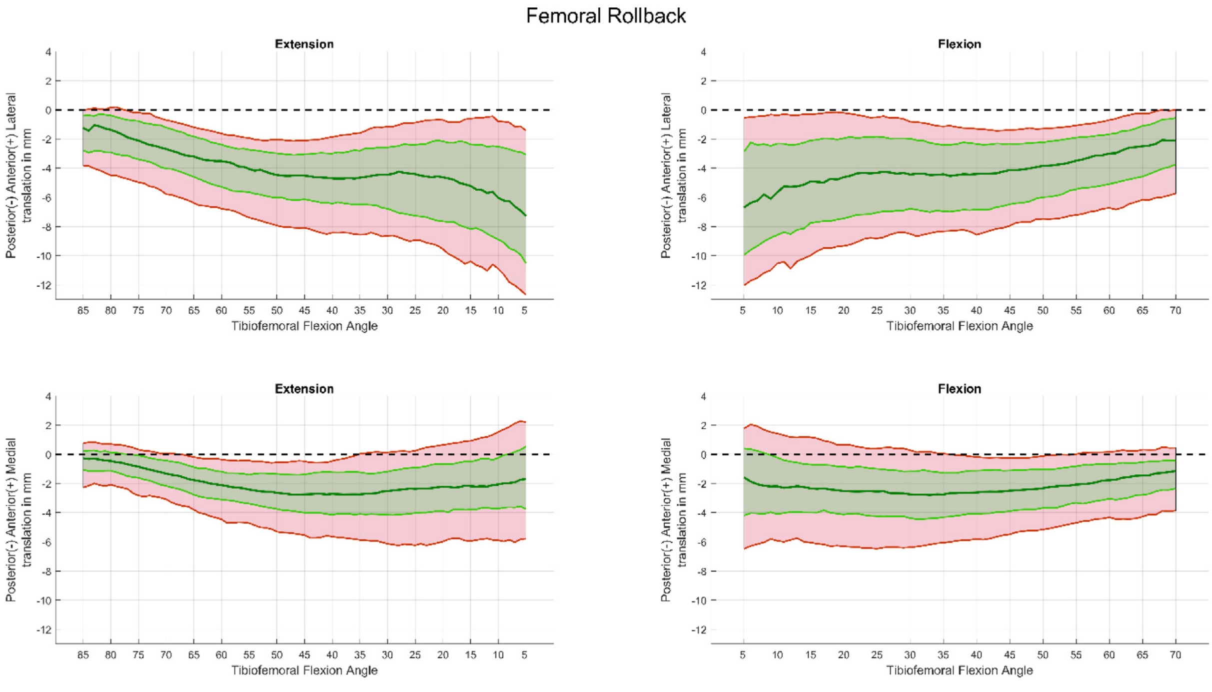

Figure 3b. Percentile plot of the femoral rollback off the lateral (upper) and medial (lower) condyle during an extension-flexion movement. (+). The horizontal axis contains the tibiofemoral flexion angle, the vertical axes are labelled To ensure smoothness and readability of the plots, measurements are only displayed between 6° and 85° of flexion, as these angles were achieved by at least 65% of all subjects.

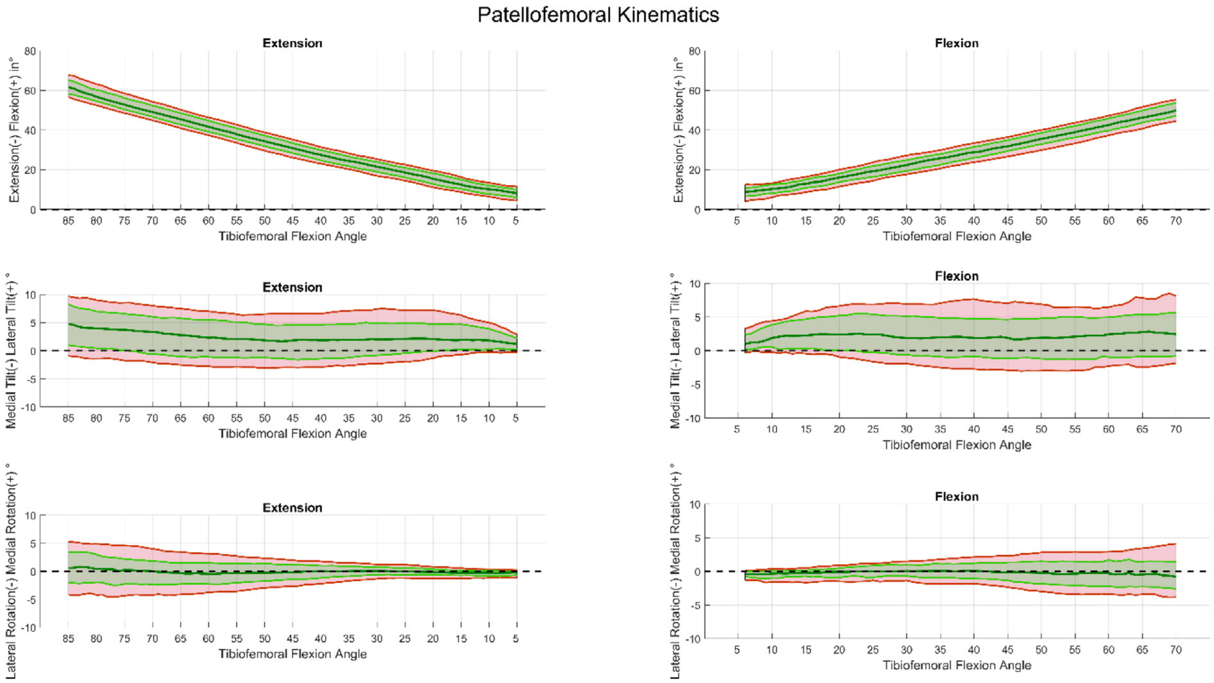

Figure 4a. Percentile plot of Patellofemoral Kinematics, green line = median green area = 25–50 percentile red area = 12.5–87.5 percentile. Top = Extension (−) Flexion (+), middle = Medial Tilt(−) Lateral Tilt(+), bottom = Lateral Rotation (−) Medial Rotation (+). The horizontal axis contains the tibiofemoral flexion angle, the vertical axes are labelled. To ensure smoothness and readability of the plots, measurements are only displayed between 6° and 85° of flexion, as these angles were achieved by at least 65% of all subjects.

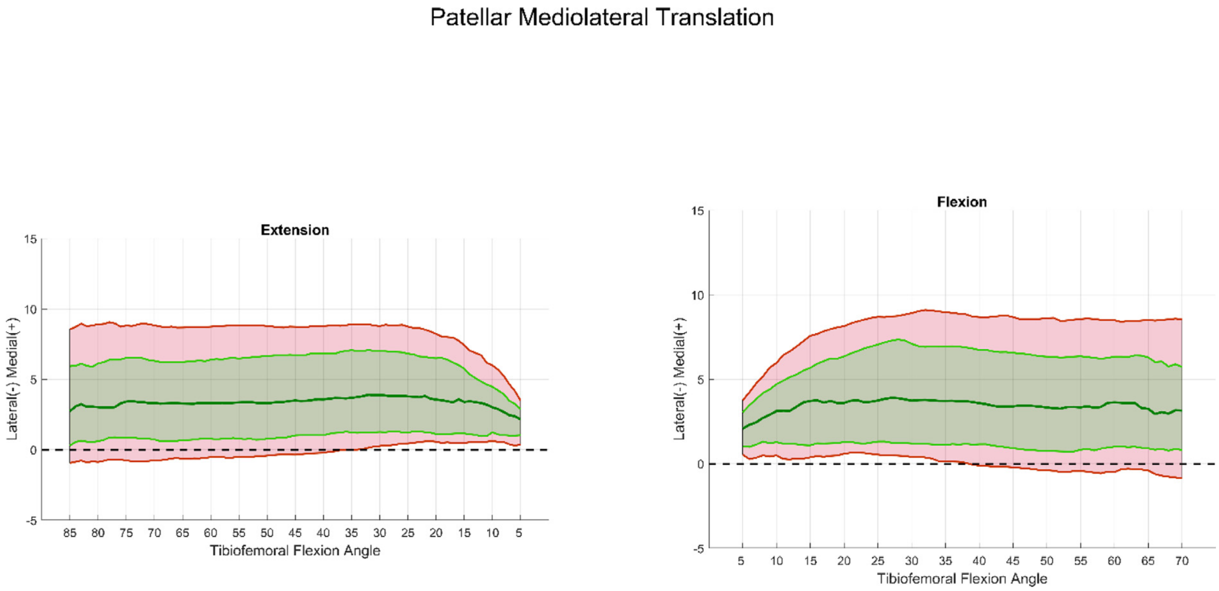

Figure 4b. Percentile plot of the mediolateral translation of the patella with respect to the femur during an extension-flexion movement. (+). The horizontal axis contains the tibiofemoral flexion angle, the vertical axes are labelled. To ensure smoothness and readability of the plots, measurements are only displayed between 6° and 85° of flexion, as these angles were achieved by at least 65% of all subjects.

4. Discussion

In-vivo patient specific dynamic assessment of knee kinematics has the potential to expand upon static measurements in the diagnosis and quantification of knee disorders and to determine the effect of orthopaedic interventions. Despite previous studies showing the usefulness of dynamic imaging and providing valuable insights in knee kinematics, dynamic imaging is not widely used in clinics. In the current study we introduce a fully automatic analysis method to extract tibiofemoral and patellofemoral kinematics and applied it to a cohort of 97 healthy subjects to establish normative knee kinematics as a reference for the analysis of knee joint pathology.

Dynamic CT imaging allows for a combination of high spatial- and temporal resolution over a large range of motion compared to other modalities. For example, compared to dynamic MRI where spatial and temporal resolution are a trade-off and flexion range is limited by the MR coil [21].

The protocol involves a simple, single movement which does not require repetitions nor specific timing, which makes it feasible for subjects with painful knees. Together with the fast automatic analysis this makes the presented methods suitable for use in daily clinical practice. As the effective radiation dose (0.08 mSv) is low compared to natural background radiation and routine CT, it is broadly applicable at relatively low-risk.

The current study presents TF and PF kinematic data of 97 healthy individuals, providing a unique dataset of normative knee kinematics. Unfortunately there is no gold standard regarding dynamic imaging to which the results of this study can be compared. However, the kinematics found in the current study are highly similar to those reported in literature. Internal and external rotation of the tibia in the studies by Seisler- and Sheehan et al. is highly comparable to the current study. In all cases there is small internal rotation with increasing flexion angle, especially in the first 30°, which can be attributed to the screw home mechanism [4,5]. Similarly, a publication by Shandiz et al. studying changes in knee kinematics after total knee arthroplasty (TKA), shows a comparable internal tibial rotation in participants prior to TKA [22].

Whereas there is little to no valgus rotation of the tibia in the studies of Seisler & Sheehan, our data suggests a median varus alignment of 5° at 85° of TF flexion. This difference may be caused by the use of different coordinate systems, where a valgus rotated, or externally rotated femoral ML axis causes a more valgus description during knee flexion [23].

Similarly to what is found in other studies, femoral rollback is larger at the lateral condyle than the medial condyle, as a result of medial pivoting [24,25]. Moreover, despite differences in loading conditions, movement task and range of motion, both magnitude and path of the medial and lateral condyle show large resemblance with the study from Gray et al. [20]. This study investigated joint motion with biplane fluoroscopy during normal walking, and found mean posterior translations of ±5 mm for the lateral condyle and ±2.5 mm for the medial condyle as well as a short period of anterior movement of the medial condyle starting around 20° of TF flexion, similar to our results.

In addition to similar tibiofemoral kinematics, patellofemoral kinematics in this study is also highly similar to aforementioned studies. Patellofemoral flexion is nearly identical during flexion and extension movement, and has a constant variation around the median of approximately 5°.

The patellar tilt shows an increase in the first 30° of tibiofemoral flexion, followed by a very subtle decrease. This initial increase may be caused by contraction of the quadriceps, causing a lateral pull on the patella. Around 20° of tibiofemoral flexion the medial facet of lateral wall of the trochlea comes into contact with the lateral facet of the patella, causing a small medial tilt. Both the median and variance (percentiles) show large similarity to Esfandiarpour and Amis et al. [3,19].

Patellar rotation is centered around zero, similar to Sheehan-, Seisler- and Amis et al. [4,5,19]. Here we see differences with the study of Esfandiarpour, which shows a medial patellar rotation of approximately 5°.

The patella shows a lateral movement of the patella during extension and at TF flexion angles smaller than ±30°, at which the patella moves out of the femoral trochlea. In literature, the mediolateral displacement of the patella is calculated and visualized in many different ways. For example, Tanaka et al. used the bisect offset which determines the fraction of the patella lateral of the femoral trochlear groove [26]. Suzuki et al. who used dual fluoroscopy to establish patellar tracking used displacement of the patellar origin with respect to the femoral origin, similar to Amis et al. and the current study [27]. In a comprehensive literature review, Yu et al. compared patellofemoral joint kinematics of 12 studies using different techniques and modalities. That study showed that there is a large variability in patellar ML translation among different studies and indicates that different movement tasks, loading conditions and analysis methods have a substantial impact on measured displacement.

Overall, our data shows that there is considerable variance in knee kinematics even within a healthy population. This variation should be taken into account when comparing patients and healthy subjects, as it may complicate distinguishing the two at an individual level. The amount of variation at a specific flexion angle is related to the angle at which rotations around the SI, and AP axis were negated and are therefore specific to this study. In case of the translations, part of the variation can be explained by knee size differences, where larger knees show more translation than smaller knees. Some studies use the epicondylar width in an attempt to negate size differences. We have not chosen to do so in the current study, as the validity of this method is unclear.

Both tibiofemoral and patellofemoral kinematics show small differences for the extension and flexion movement. As this difference is most pronounced in patellofemoral kinematics, this may be a result of concentric versus eccentric contraction of the quadriceps muscle. It may therefore be necessary to consider these movements separately.

There are limitations of this study that should be considered. First, is the negation of the offsets in rotation and translation of both tibia and patella at the lowest TF flexion angle. This assumes full alignment of the patellar and tibial ML and AP axes with those of the femur at the smallest flexion angle (i.e. extension), where in practice this is not the case. Due to a natural variation in pose and anatomy, there will be a range of different starting-positions and -orientations. The variations in kinematics are highly dependent on the flexion angle at which rotations around the SI and AP axis were negated and from this cannot be concluded that higher flexion angles are associated with larger variance in kinematics. Furthermore, as not every subject was able to reach 0° of TF flexion, negation of rotations and translations at the smallest TF angle will introduce variations. However, the introduced variations as a result of negating rotations will be small and have no effect on the calculated median and percentiles. Moreover, the current approach allows us to solely investigate movements relative to the extended position, rather than a combination of movement and different starting positions and orientations.

Secondly, the choice of coordinate system has a major influence on the kinematic description [8,16,28,29]. The choice of coordinate system together with natural variation in anatomy and pose are a possible explanation for offsets, or different starting positions and orientations [23]. The absolute numbers from this study, may therefore not by directly comparable to studies where other coordinate systems are used. Negating the data, may reduce these differences. Moreover, as was previously mentioned, differences with other studies are small and trends are similar and movement patterns of the tibia as well as the patella relative to the femur are similar to those reported in the literature.

Lastly, it is known that knee kinematics are different for different tasks and loading conditions. A flexion extension movement is not a challenging or error-prone movement. Episodes of, for example, instability of the knee joint will therefore most likely not occur during the scan as these are usually associated with weightbearing activities. It is unclear whether the occurrence of such episodes is necessary for a better understanding of the underlying cause, and the same applies for other knee disorders. Knee kinematics are dependent on loading conditions. In this study, data were gathered under non-weightbearing conditions. For example, varus/valgus rotation is significantly different in a weightbearing versus non-weightbearing situation [30]. As a result, values found in this study cannot be extrapolated to a weightbearing situation. Interestingly, multiple studies have found that tibiofemoral and patellofemoral rotations and translations are more pronounced in non-weightbearing versus weightbearing conditions [31–33]. Due to large forces acting on the knee joint during weightbearing, the effect of smaller, less powerful but important structures for knee kinematics such as the MPFL, Iliotibial band or lateral retinaculum may be less apparent. Therefore, a flexion extension movement against gravity might provide better insight into the more subtle aspects of knee kinematics, and therefore kinematic disorders. The presented method of real-time dynamic CT-scanning proved to be easily applicable in a clinical setting. Although not all CT scanners are capable of dynamic imaging, it has a large potential to investigate numerous knee disorders in vivo. Dynamic imaging and associated image analysis offers a new set of challenges. Applying existing measurements made for static imaging to dynamic imaging data can have results that are counterintuitive or difficult to explain. To fully exploit these techniques, existing dogmas and static measurements should therefore be reconsidered, and new diagnostic methods must be developed. These automatized, 3D, dynamic methods will therefore likely change the personalized diagnostic capacity for patients with knee pathologies and will further optimize treatment options and evaluation methods in order to improve patient care.

Declaration of Competing Interest

The authors declare that they have no known competing financial interests or personal relationships that could have appeared to influence the work reported in this paper.

References

[1] Katchburian MV, Bull AMJ, Shih YF, Heatley FW, Amis AA. Measurement of patellar tracking: Assessment and analysis of the literature. Clin Orthop Relat Res 2003;412:241–59. doi: https://doi.org/10.1097/01.blo.0000068767.86536.9a.
[2] Rosa SB, Ewen PM, Doma K, Ferrer JFL, Grant A. Dynamic evaluation of patellofemoral instability: a clinical reality or just a research field? A Literature review. Orthop Surg 2019;11:932–42. doi: https://doi.org/10.1111/os.12549.
[3] Esfandiarpour F, Lebrun CM, Dhillon S, Boulanger P. In-vivo patellar tracking in individuals with patellofemoral pain and healthy individuals. J Orthop Res 2018;36:2193–201. doi: https://doi.org/10.1002/jor.23887.
[4] Seisler AR, Sheehan FT. Normative three-dimensional patellofemoral and tibiofemoral kinematics: A dynamic, in vivo study. IEEE Trans Biomed Eng 2007;54:1333–41. doi: https://doi.org/10.1109/TBME.2007.890735.
[5] Sheehan FT, Derasari A, Brindle TJ, Alter KE. Understanding patellofemoral pain with maltracking in the presence of joint laxity: Complete 3D in vivo patellofemoral and tibiofemoral kinematics. J Orthop Res 2009;27:561–70. doi: https://doi.org/10.1002/jor.20783.
[6] Elias JJ, Carrino JA, Saranathan A, Guseila LM, Tanaka MJ, Cosgarea AJ. Variations in kinematics and function following patellar stabilization including tibial tuberosity realignment. Knee Surg Sports Traumatol Arthrosc 2014;22:2350–6. doi: https://doi.org/10.1007/s00167-014-2905-9.
[7] Salsich GB, Perman WH. Patellofemoral joint contact area is influenced by tibiofemoral rotation alignment in individuals who have patellofemoral pain. J Orthop Sports Phys Ther 2007;37:521–8. doi: https://doi.org/10.2519/jospt.2007.37.9.521.
[8] Yu Z, Yao J, Wang X, Xin X, Zhang K, Cai H, et al. Research methods and progress of patellofemoral joint kinematics: a review. J Healthc Eng 2019;2019. doi: https://doi.org/10.1155/2019/9159267.
[9] Zhao K, Breighner R, Holmes D, Leng S, McCollough C, An K-N. A technique for quantifying wrist motion using four-dimensional computed tomography: approach and validation. J Biomech Eng 2015;137:. doi: https://doi.org/10.1115/1.4030405074501.
[10] Adachi T. Accuracy Verification of 4D-CT Analysis of Knee Joint Movements: A Pilot Study Using a Knee Joint Model and Motion-capture System 2021:1–14.
[11] Li X, Chen H, Qi X, Dou Q, Fu CW, Heng PA. H-DenseUNet: Hybrid Densely Connected UNet for Liver and Tumor Segmentation from CT Volumes. IEEE Trans Med Imaging 2018;37:2663–74. doi: https://doi.org/10.1109/TMI.2018.2845918.
[12] Tran AP, Yan S, Fang Q. Improving model-based functional near-infrared spectroscopy analysis using mesh-based anatomical and light-transport models. Neurophotonics 2020;7:1. doi: https://doi.org/10.1117/1.nph.7.1.015008.
[13] Myronenko A, Song X. Point set registration: Coherent point drifts. IEEE Trans Pattern Anal Mach Intell 2010;32:2262–75. doi: https://doi.org/10.1109/TPAMI.2010.46.
[14] Klein S, Staring M, Murphy K, Viergever MA, Pluim J. <emphasis emphasistype=“mono”>elastix</emphasis>: A Toolbox for Intensity-Based Medical Image Registration. IEEE Trans Med Imaging 2010;29:196–205.
[15] Miranda DL, Rainbow MJ, Leventhal EL, Crisco JJ, Fleming BC. Automatic determination of anatomical coordinate systems for three-dimensional bone models of the isolated human knee. J Biomech 2010;43:1623–6. doi: https://doi.org/10.1016/j.jbiomech.2010.01.036.

[16] Dunning H, van de Groes SAW, Verdonschot N, Buckens CF, Janssen D. The sensitivity of an anatomical coordinate system to anatomical variation and its effect on the description of knee kinematics as obtained from dynamic CT imaging. Med Eng Phys 2022;102:. doi: https://doi.org/10.1016/j.medengphy.2022.103781103781.
[17] Chen H, Kluijtmans L, Bakker M, Dunning H, Kang Y, Sebastiaan vdG, et al. A robust and semi-automatic quantitative measurement of patellofemoral instability based on 4D computed tomography; n.d.
[18] Grood ES, Suntay WJ. A joint coordinate system for the clinical description of three-dimensional motions: Application to the knee. J Biomech Eng 1983;105:136–44. doi: https://doi.org/10.1115/1.3138397.
[19] Amis AA, Senavongse W, Bull AMJ. Patellofemoral Kinematics during Knee Flexion-Extension : An In Vitro Study. J Orthop Res 2006;24:2201–11. doi: https://doi.org/10.1002/jor.20268.
[20] Gray HA, Guan S, Thomeer LT, Schache AG, de Steiger R, Pandy MG. Three-dimensional motion of the knee-joint complex during normal walking revealed by mobile biplane x-ray imaging. J Orthop Res 2019;37:615–30. doi: https://doi.org/10.1002/jor.24226.
[21] Garetier M, Borotikar B, Makki K, Brochard S, Rousseau F, Ben SD. Dynamic MRI for articulating joint evaluation on 1.5 T and 3.0 T scanners: setup, protocols, and real-time sequences. Insights. Imaging 2020:11. doi: https://doi.org/10.1186/s13244-020-00868-5.
[22] Akbari Shandiz M, Boulos P, Saevarsson SK, Yoo S, Miller S, Anglin C. Changes in knee kinematics following total knee arthroplasty. Proc Inst Mech Eng Part H J Eng Med 2016;230:265–78. doi: https://doi.org/10.1177/0954411916632491.
[23] Lenz NM, Mane A, Maletsky LP, Morton NA. The effects of femoral fixed body coordinate system definition on knee kinematic description. J Biomech Eng 2008;130:1–7. doi: https://doi.org/10.1115/1.2898713.
[24] Von Eisenhart-Rothe R, Lenze U, Hinterwimmer S, Pohlig F, Graichen H, Stein T, et al. Tibiofemoral and patellofemoral joint 3D-kinematics in patients with posterior cruciate ligament deficiency compared to healthy volunteers. BMC Musculoskelet Disord 2012:13. doi: https://doi.org/10.1186/1471-2474-13-231.
[25] Pinskerova V, Johal P, Nakagawa S, Sosna A, Williams A, Gedroyc W, et al. Does the femur roll-back with flexion? J Bone Jt Surg - Ser B 2004;86:925–31. doi: https://doi.org/10.1302/0301-620X.86B6.14589.
[26] Tanaka MJ, Elias JJ, Williams AA, Demehri S, Cosgarea AJ. Characterization of patellar maltracking using dynamic kinematic CT imaging in patients with patellar instability. Knee Surgery, Sport Traumatol Arthrosc 2016;24:3634–41. doi: https://doi.org/10.1007/s00167-016-4216-9.
[27] Suzuki T, Hosseini A, Li JS, Gill TJ, Li G. In vivo patellar tracking and patellofemoral cartilage contacts during dynamic stair ascending. J Biomech 2012;45:2432–7. doi: https://doi.org/10.1016/j.jbiomech.2012.06.034.
[28] Kedgley AE, McWalter EJ, Wilson DR. The effect of coordinate system variation on in vivo patellofemoral kinematic measures. Knee 2015;22:88–94. doi: https://doi.org/10.1016/j.knee.2014.11.006.
[29] Grant C, Fick CN, Welsh J, McConnell J, Sheehan FT. A Word of Caution for Future Studies in Patellofemoral Pain: A Systematic Review With Meta-analysis. Am J Sports Med 2021;49:538–51. doi: https://doi.org/10.1177/0363546520926448.
[30] Fritz B, Fritz J, Fucentese SF, Pfirrmann CWA, Sutter R. Three-dimensional analysis for quantification of knee joint space width with weight-bearing CT: comparison with non-weight-bearing CT and weight-bearing radiography. Osteoarthr Cartil 2022;30:671–80. doi: https://doi.org/10.1016/j.joca.2021.11.019.
[31] Draper CE, Besier TF, Fredericson M, Santos JM, Gary S, Delp SL, et al. Differences in Patellofemoral Kinematics between Weight- Bearing and Non-Weight-Bearing Conditions in Patients with Patellofemoral Pain. J Orthop Res 2010;29:312–7. doi: https://doi.org/10.1002/jor.21253.
[32] Victor J, Labey L, Wong P, Innocenti B, Bellemans J. The influence of muscle load on tibiofemoral knee kinematics. J Orthop Res 2010;28:419–28. doi: https://doi.org/10.1002/jor.21019.
[33] Souza RB, Draper CCE, Fredericson M, Powers MDCM. Femur Rotation and Patellofemoral Joint Kinematics: A Weight-Bearing Magnetic Resonance Imaging. Analysis 2010;40:277–85. doi: https://doi.org/10.2519/jospt.2010.3215.